Int. J. Solids Structures Vol. 17, No. 10, pp. 961–967, 1981
Printed in Great Britain.

0020-7683/81/100961-07$02.00/0

A TIME-INDEPENDENT ANALYSIS FOR THE FINAL STATE OF AN ELASTO-VISCO-PLASTIC MEDIUM WITH INTERNAL CAVITIES

TAIJIRO NONAKA
Disaster Prevention Research Institute, Kyoto University, Uji City, Kyoto Prefecture, Japan

(*Received* 26 *August* 1980; *in revised form* 13 *January* 1981)

Abstract—It is supposed that a spherical or circular-cylindrical cavity is bored in an infinite hydrostatic field. Space and time variation of stress was determined in a previous paper on the basis of an elasto-visco-plastic four-element model of distortional material behavior. It was assumed that a rigid wall was installed in contact with the cavity surface instantaneously upon boring. In the present paper the effects of wall deformability and delayed installation are taken into account in determining the final state attained when viscous action terminates. A simple closed form solution is derived from a time-independent analysis of linear elasticity followed by linear work-hardening. The interpretation of the time-independent solution as representing the final state justifies classical elastic or elastic-plastic analyses in the viscosity-dependent problems of tunnels and underground structures.

NOTATION

b radius of elastic-inelastic boundary
G modulus of shear rigidity
k yield stress in shear
p pressure
R radius of cavity
r radial coordinate
t time
U inward displacement of cavity surface
u radial displacement
γ shear strain
ϵ extensional strain
η coefficient of viscosity
μ modulus of shear rigidity
σ tensile stress

Subscripts
r radial component
z axial component
θ circumferential component
0 cavity excavation
1 wall installation
∞ final state

INTRODUCTION

Rational proportioning of lining around a tunnel or underground opening requires the determination of the load exerted by the earth. Based on a four-element model, a closed-form solution has been derived in a previous paper on the elasto-visco-plastic stress distribution in the vicinity of a cavity of a sphere or circular cylinder[1]. It has been assumed that the cavity is bored in an infinite hydrostatic field and strengthened instantaneously by installing a surrounding wall of infinite rigidity. Spontaneous elastic response upon boring is followed by a stress relaxation phenomenon and a surface traction develops, in the course of time, acting on the wall as a load, which becomes maximum when viscous action terminates. However, both deformability of the wall and delayed installation influence the stress distribution, reducing the load. It is the objective of this paper to examine and incorporate these effects in the analysis to determine the final state; a simple closed-form solution of the viscosity independent final state is of much practical use in civil and mining engineering. Salamon discusses the design of a circular tunnel on the basis of elasto-visco-plastic mathematical models of different kinds. This reference has been brought to the author's attention since the completion of his previous paper and should be included in its literature on time-dependent analyses[2].

A time-independent analysis suffices to determine the final state. The analysis does not distinguish the problem in question from the circumstance where an elastic–plastic medium with an internal cavity is subjected to radial loading at a distance and hence is applicable to that circumstance. The analysis simulates a body of a structure or structural member which is perforated, is strengthened and carries a load. It is worth noting that the interpretation of the results of a time-independent analysis as representing the final state of a viscosity dependent medium justifies the application of classical elastic[3] or elastic–plastic[4] approaches to the problems of underground excavations; those approaches are unable to account for the actual order of loading, boring and installation.

ASSUMPTIONS AND KINEMATIC RELATIONS

A cavity of a sphere (case a) or of a circular cylinder (case b) with radius R is assumed to be bored just prior to time $t = 0$ in an infinite medium which is under constant hydrostatic pressure p. The medium is supposed to be incompressible, uniform and isotropic and its distortional behavior is represented by the four-element model of Fig. 1. It is composed of a linear spring with modulus of rigidity G in series with the parallel combination of a linear spring with modulus of rigidity μ, a Newtonian dashpot with coefficient of viscosity η and a perfectly plastic slider. The slider is free from the influence of hydrostatic pressure and yields under tensile stress $2k$ in case a and under shear stress k in case b. In order to apply the analysis to the case of all-around tension instead of hydrostatic pressure, it is only necessary to replace p and k by $-p$ and $-k$, respectively. Among other assumptions are isothermal condition, small deformation, and absence of body force. It follows from spherical symmetry in case a that the radial and any two tangential directions are principal directions so that the components $(\sigma_r, \sigma_\theta, \sigma_\theta)$ of stress and $(\epsilon_r, \epsilon_\theta, \epsilon_\theta)$ of strain are their principal values (Fig. 3(a)). Similarly, from cylindrical symmetry the components $(\sigma_r, \sigma_\theta, \sigma_z)$ and $(\epsilon_r, \epsilon_\theta, \epsilon_z)$ are the principal stresses and strains, respectively, in case b, where plane strain $\epsilon_z = 0$ is assumed (Fig. 3(b)).

Both cases are analysed in parallel, with a, b, or nothing annexed to the numbers of equations and figures referring to the case a, b, or both, respectively. Displacement u occurring along the radius r determines strain components through $\epsilon_r = u'$ and $\epsilon_\theta = u/r$, where the prime denotes differentiation with respect to r. By taking the incompressibility into consideration, it is seen that

$$u(r, t) = -U\frac{R^2}{r^2}, \qquad u(r, t) = -U\frac{R}{r}, \tag{1a, b}$$

where $U(t)$ is the radial inward displacement at the cavity surface. The locally greatest shearing strain

$$\gamma(r, t) = \epsilon_r - \epsilon_\theta = r\left(\frac{u}{r}\right)' \tag{2}$$

attains the yield point strain k/G at $r = b(t)$ for U large enough to satisfy the inequality $b/R \geqq 1$, where

$$\frac{b^3}{R^3} = 3\frac{GU}{kR}, \qquad \frac{b^2}{R^2} = 2\frac{GU}{kR}. \tag{3a, b}$$

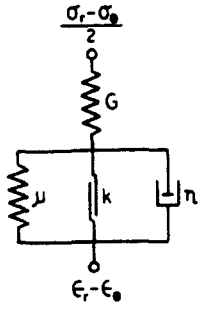

Fig. 1. Four-element model.

PREVIOUS RESULTS

Spontaneous boring is accompanied by elastic response as shown in the distortional stress-strain relationship of Fig. 2 by line OS, which can be thought of as representing a continually distributed radius with the origin O corresponding to $r=\infty$, the point S to $r=R$, and intermediate point E to $r=b$. If a rigid wall is installed in intimate contact with the cavity surface at $t=0$ immediately upon boring, then the deformation is kept constant with

$$U(t)=U(0)\equiv U_0; \qquad b(t)=b(0)\equiv b_0, \tag{4}$$

where

$$\frac{U_0}{R}=\frac{p}{4G}, \qquad \frac{U_0}{R}=\frac{p}{2G}; \tag{5a, b}$$

$$\frac{b_0^3}{R^3}=\frac{3p}{4k}, \qquad \frac{b_0^2}{R^2}=\frac{p}{k}. \tag{6a, b}$$

While the elastic region $b_0 \leqq r<\infty$ is under constant stress, the inelastic region $R \leqq r \leqq b_0$ undergoes stress relaxation and a point such as S in Fig. 2 moves vertically downward toward the final point F on the work-hardening relation EH[1]. For $t \geqq 0$ the radial stress has been determined to vary as

$$\sigma_r(r,t)=\begin{cases} -p+\dfrac{4k}{3}\dfrac{G}{G+\mu}\left[1+\dfrac{\mu}{G}\dfrac{b_0^3}{r^3}+\ln\dfrac{b_0^3}{r^3}+\left(\dfrac{b_0^3}{r^3}-1-\ln\dfrac{b_0^3}{r^3}\right)e^{-[(G+\mu)/\eta]t}\right] \\ \qquad\qquad \text{for} \quad R \leqq r \leqq b_0 \\ -p\left(1-\dfrac{R^3}{r^3}\right) \qquad \text{for} \quad b_0 \leqq r<\infty \end{cases} \tag{7a}$$

$$\sigma_r(r,t)=\begin{cases} -p+k\dfrac{G}{G+\mu}\left[1+\dfrac{\mu}{G}\dfrac{b_0^2}{r^2}+\ln\dfrac{b_0^2}{r^2}+\left(\dfrac{b_0^3}{2r^3}-\dfrac{1}{2}+\ln\dfrac{b_0^3}{r^3}\right)e^{-[(G+\mu)/\eta]t}\right] \\ \qquad\qquad \text{for} \quad R \leqq r \leqq b_0 \\ -p\left(1-\dfrac{R^2}{r^2}\right) \qquad \text{for} \quad b_0 \leqq r<\infty \end{cases} \tag{7b}$$

and the circumferential stress

$$\sigma_\theta(r,t)=\begin{cases} -p-\dfrac{4k}{3}\dfrac{G}{G+\mu}\left[\dfrac{1}{2}+\dfrac{\mu}{2G}\dfrac{b_0^3}{r^3}-\ln\dfrac{b_0^3}{r^3}+\left(\dfrac{b_0^3}{r^3}-1-\ln\dfrac{b_0^3}{r^3}\right)e^{-[(G+\mu)/\eta]t}\right] \\ \qquad\qquad \text{for} \quad R \leqq r \leqq b_0 \\ -p\left(1+\dfrac{R^3}{2r^3}\right) \qquad \text{for} \quad b_0 \leqq r<\infty \end{cases} \tag{8a}$$

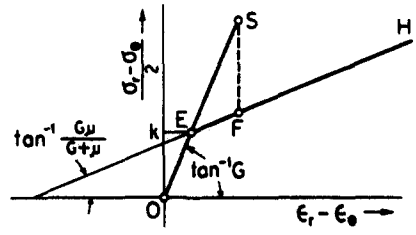

Fig. 2. Distortional stress–strain relation.

$$\sigma_\theta(r,t)=\begin{cases}-p-k\dfrac{G}{G+\mu}\left[1+\dfrac{\mu}{G}\dfrac{b_0^2}{r^2}-\ln\dfrac{b_0^2}{r^2}+\left(\dfrac{b_0^2}{r^2}-1+\ln\dfrac{b_0^2}{r^2}\right)e^{-[(G+\mu)/\eta]t}\right] & \\ \qquad\qquad \text{for} \quad R\leqq r\leqq b_0 & \\ -p\left(1+\dfrac{R^2}{r^2}\right) \qquad \text{for} \quad b_0\leqq r<\infty, & \end{cases} \tag{8b}$$

The axial stress for case b is given throughout by $\sigma_z=(\sigma_r+\sigma_\theta)/2$. It is clear from eqn (6) that if p is so small that

$$\frac{3p}{4k}\leqq 1, \qquad \frac{p}{k}\leqq 1, \tag{9a, b}$$

then no inelastic action is involved and the wall, when installed, would not be exposed to any load. Thus, such cases as shown by eqn (9) are excluded in the subsequent discussions, because of their triviality.

TIME-INDEPENDENT ANALYSIS

If the wall is deformable or has not been installed, not only stress varies but deformation keeps growing with increasing $U(t)$. It is accompanied by increasing $b(t)$ according to eqn (3). It is seen from eqn (1) to eqn (3) that distortion also progresses according to

$$\gamma(r,t)=\frac{k}{G}\frac{b^3}{r^3}, \qquad \gamma(r,t)=\frac{k}{G}\frac{b^2}{r^2}, \tag{10a, b}$$

while equilibrium

$$\sigma_\theta=\sigma_r+\frac{r}{2}\sigma_r'=\frac{1}{2r}(r^2\sigma_r)', \tag{11a}$$

$$\sigma_\theta=\sigma_r+r\sigma_r'=(r\sigma_r)' \tag{11b}$$

is maintained.

Elastic behavior pervades the region $b\leqq r<\infty$, for which the absence of previous inelastic straining ensures the constitutive relation

$$\sigma_r-\sigma_\theta=2G(\epsilon_r-\epsilon_\theta). \tag{12}$$

Upon substitution of eqns (1)–(3) and (11) this is integrated with respect to r under the boundary condition $\sigma_r(\infty,t)=-p$ to give

$$\sigma_r(r,t)=\frac{4k}{3}\frac{b^3}{r^3}-p, \qquad \sigma_r(r,t)=k\frac{b^2}{r^2}-p. \tag{13a, b}$$

Equations (11) and (13) are combined to give

$$\sigma_\theta(r,t)=-\frac{2k}{3}\frac{b^3}{r^3}-p, \qquad \sigma_\theta(r,t)=-k\frac{b^2}{r^2}-p. \tag{14a, b}$$

In case b the assumptions of incompressibility and plane strain provide $\sigma_z=(\sigma_r+\sigma_\theta)/2$. It is noted that the stresses vary with time as the elastic-inelastic boundary moves in accordance with eqn (3).

In the region $R\leqq r\leqq b$, the viscous and plastic elements are activated in Fig. 1 together with the elastic springs. In view of the growing distortion, it is seen that a point such as S in Fig. 2 moves in a direction which has a positive horizontal component, depending on the property of the wall installed, which may also behave in an elasto–visco–plastic manner. The point finally settles down somewhere on the line segment FH. Determination is made of the final state by an

elastic–plastic analysis, valid whether viscosity be linear or nonlinear. It is supposed that in the final state the wall exerts on the cavity surface a reaction $-\sigma_r(R,\infty)$, which is a function of the final surface displacement. Negligence of the dashpot in Fig. 1 furnishes the constitutive relation of linear work-hardening

$$\left(1+\frac{\mu}{G}\right)(\sigma_r-\sigma_\theta)=2\mu(\epsilon_r-\epsilon_\theta)+2k. \tag{15}$$

This is combined with eqns (1)–(3) and (11) to give

$$\sigma_r'(r,\infty)=\frac{G}{G+\mu}\left[\frac{4\mu k}{3G}\left(\frac{b_\infty^3}{r^3}\right)'-\frac{4k}{r}\right], \tag{16a}$$

$$\sigma_r'(r,\infty)=\frac{G}{G+\mu}\left[\frac{\mu k}{G}\left(\frac{b_\infty^2}{r^2}\right)'-\frac{2k}{r}\right], \tag{16b}$$

where the symbol ∞ in the subscripts indicates final values. Integration from $r=r$ to $r=b_\infty$, at which use is made of the continuity with the elastic solution eqn (13), gives

$$\sigma_r(r,\infty)=-p+\frac{4k}{3}\frac{G}{G+\mu}\left[1+\frac{\mu}{G}\frac{b_\infty^3}{r^3}+\ln\frac{b_\infty^3}{r^3}\right], \tag{17a}$$

$$\sigma_r(r,\infty)=-p+k\frac{G}{G+\mu}\left[1+\frac{\mu}{G}\frac{b_\infty^2}{r^2}+\ln\frac{b_\infty^2}{r^2}\right]. \tag{17b}$$

Equations (11) and (17) are combined to give

$$\sigma_\theta(r,\infty)=-p-\frac{4k}{3}\frac{G}{G+\mu}\left[\frac{1}{2}+\frac{\mu}{2G}\frac{b_\infty^3}{r^3}-\ln\frac{b_\infty^3}{r^3}\right], \tag{18a}$$

$$\sigma_\theta(r,\infty)=-p-k\frac{G}{G+\mu}\left[1+\frac{\mu}{G}\frac{b_\infty^2}{r^2}-\ln\frac{b_\infty^2}{r^2}\right]. \tag{18b}$$

The relation

$$\sigma_z=\frac{\sigma_r+\sigma_\theta}{2} \tag{19b}$$

in case b follows from its validity at $t=0$ and the continued validity of its incremental relation† up to $t=\infty$. The boundary radius b_∞ is determined from the boundary condition ar $r=R$, depending upon the wall deformability. Suppose, for example, that the wall is linear with stiffness s so that

$$-\sigma_r(R,\infty)=s(U_\infty-U_1), \tag{20}$$

where U_1 designates the inward displacement of the cavity surface at the initiation of its intimate contact with the wall; it may be the displacement at the time when the wall is installed after boring, or the wall may initially be installed inside the cavity with clearance. Combination of eqns (3), (17) and (20) furnishes the relation

$$\frac{sR}{4G}\left(\frac{b_\infty^3}{R^3}-\frac{b_1^3}{R^3}\right)+\frac{G}{G+\mu}\left(1+\frac{\mu}{G}\frac{b_\infty^3}{R^3}+\ln\frac{b_\infty^3}{R^3}\right)=\frac{3p}{4k}, \tag{21a}$$

$$\frac{sR}{2G}\left(\frac{b_\infty^2}{R^2}-\frac{b_1^2}{R^2}\right)+\frac{G}{G+\mu}\left(1+\frac{\mu}{G}\frac{b_\infty^2}{R^2}+\ln\frac{b_\infty^2}{R^2}\right)=\frac{p}{k}, \tag{21b}$$

†This is established from the flow rule associated with the hydrostatic pressure independent yield condition as before [1]. Since the state of stress with eqn (19b) is the superposition of a hydrostatic pressure and simple shear in the plane perpendicular to z-axis, strain increment $d\epsilon_z$ is elastically related with stress increments at $t=0$. It follows from the plane strain $d\epsilon_z=0$ and incompressibility that $d\sigma_z-(d\sigma_r+d\sigma_\theta)/2=0$.

where b_1 is related to U_1 through eqn (3). The values U_∞ and b_∞ become maximum when no wall is installed at all. The maximum values are determined by setting $s = 0$ in eqn (21) with the help of eqn (3), and they also set upper bounds by themselves to U_1 and b_1, whose lower bounds are U_0 and b_0, respectively, in order to be of any physical meaning. For a rigid wall, $s = \infty$, $U_\infty = U_1$ and $b_\infty = b_1$. The wall installation at $t = 0$ in contact with the cavity surface specifies $U_1 = U_0$ and $b_1 = b_0$. Specification $U_\infty = U_1 = U_0$, $b_\infty = b_1 = b_0$ confirms the coincidence of the herein derived results with the equations of the previous section in the limit $t \to \infty$.

An example is given of the distribution of stress and displacement for the case $\mu = G$, $p = 4k$ in Fig. 3(a) and (b). Plotted downward are the dimensionless quantities $-\sigma_r/p$, $-\sigma_\theta/p$ and $-(2G/p)(u/R)$ as functions of r/R. Solid lines indicate the initial state upon boring. Dashed lines and dotted lines refer to the final states attained in the absence of a wall and with a rigid wall installed in contact with the surface at $t = 0$, respectively; in the former the boundary radius changes from

$$b_0 = 1.442R, \qquad b_0 = 2R \tag{22a, b}$$

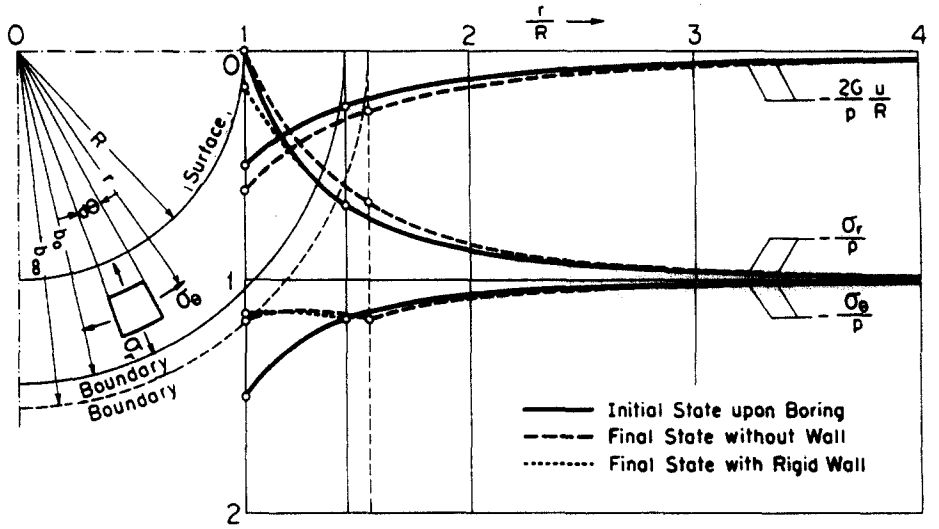

(a)

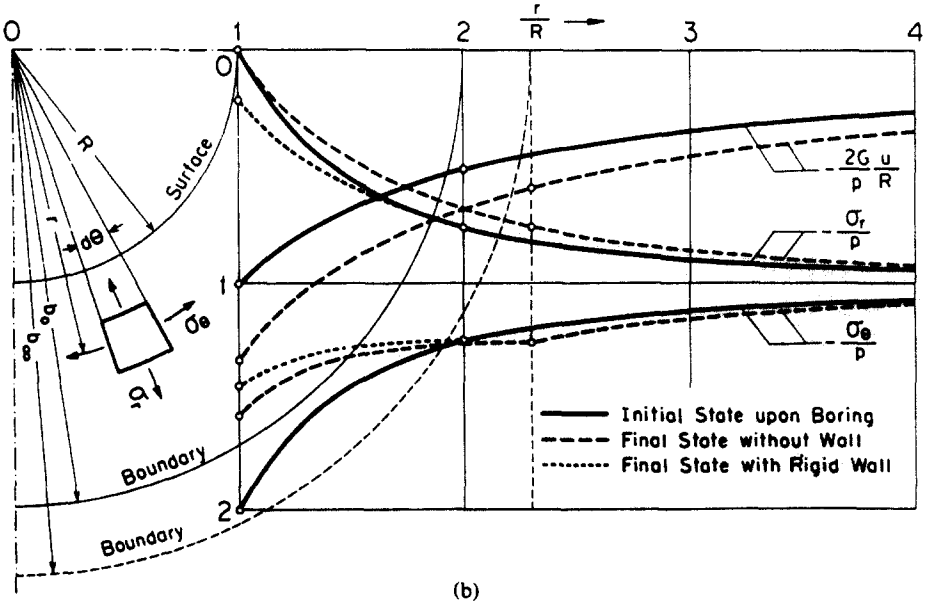

(b)

Fig. 3. Displacement and stress distribution; $\mu = G$, $p = 4k$. (a) Spherical cavity. (b) Cylindrical cavity.

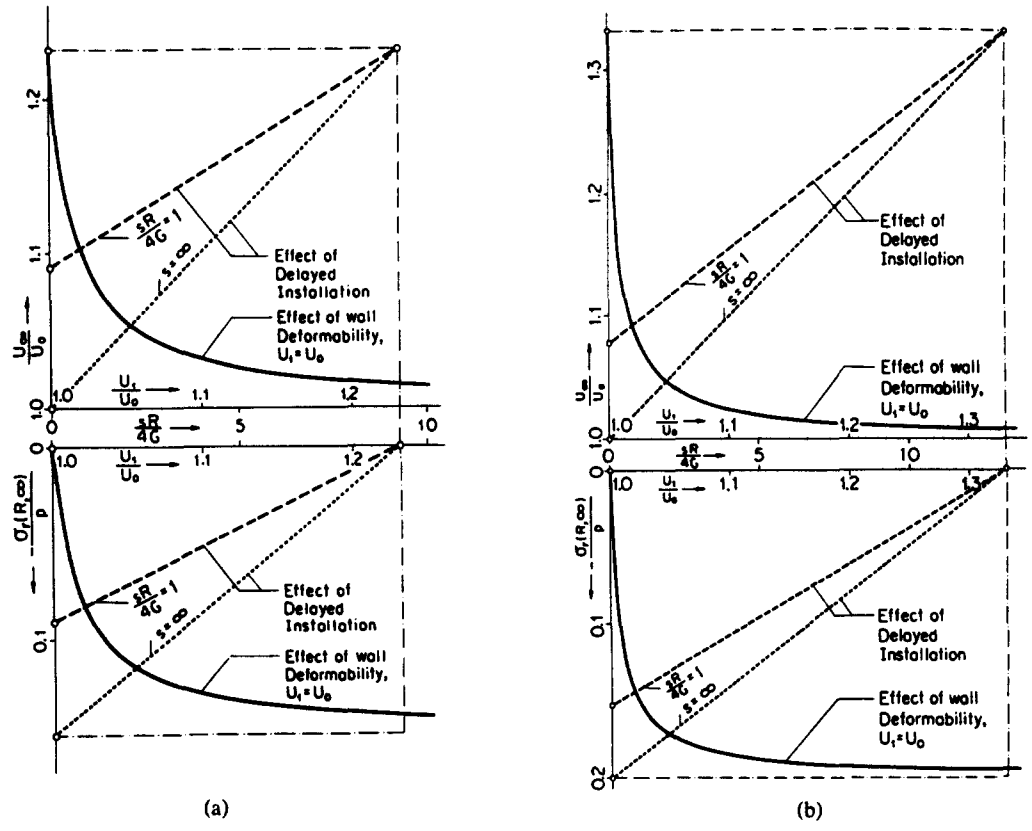

Fig. 4. Effects of wall deformability and delayed installation; $\mu = G$, $p = 4k$. (a) Spherical cavity. (b) Cylindrical cavity.

to

$$b_\infty = 1.546R, \qquad b_\infty = 2.308R, \tag{23a, b}$$

as against the constant displacement under eqn (22) in the latter.

EFFECTS OF WALL DEFORMABILITY AND DELAYED INSTALLATION

Curves are drawn in Fig. 4(a) and (b) in order to observe the effects of wall deformability (solid lines) and delayed installation (dashed lines and dotted lines) on the load (lower plots) and deformation (upper plots). It is again assumed that $\mu = G$ and $p = 4k$. The solid lines relate U_∞/U_0 and $-\sigma_r(R,\infty)/p$ to $sR/(4G)$ under condition $U_1 = U_0$, to indicate that an increase in the stiffness causes a rapid increase in the load and a rapid reduction in the deformation until $sR/(4G)$ reaches about one or two, whereas the changes are quite slow after $sR/(4G)$ exceeds about four or five. Dashed lines relate U_∞/U_0 and $-\sigma_r(R,\infty)/p$ to U_1/U_0 under condition $sR/(4G) = 1$, and dotted lines under condition $s = \infty$. It is seen that an increase in U_1 reduces the load and increases the deformation in an approximately linear manner.

Acknowledgement—The author wishes to thank Dr. Y. Kobayashi of Kyoto University Disaster Prevention Research Institute for his interest and helpful discussions during the preparation of this paper.

REFERENCES

1. T. Nonaka, An elasto-visco-plastic analysis for spherically and cylindrically symmetric problems. *Ingenieur-Archiv* 47, 27-33 (1978).
2. M. D. G. Salamon, Rock mechanics of underground excavations. Advances in rock mechanics. *Proc. 3rd Congress of the Int. Society for Rock Mechanics* Vol. I, Part B, pp. 951-1099, Denver, Colorado (1974).
3. H. Schmit, *Statische Probleme des Tunnel- und Druckstollenbaues und ihre gegenseitigen Beziehungen.* Springer, Berlin (1926).
4. H. Kastner, *Statik und Tunnel- und Stollenbaues*, 2nd Edn. Springer, Heidelberg (1971).